

# Amino Acid Based Low-Molecular-Weight Ionogels as Efficient Dye-Adsorbing Agents and Templates for the Synthesis of TiO<sub>2</sub> Nanoparticles

Sounak Dutta, Dibyendu Das, Antara Dasgupta, and Prasanta Kumar Das\*<sup>[a]</sup>

**Abstract:** The gelation of ionic liquids is attracting significant attention because of its large spectrum of applications across different disciplines. These 'green solvents' have been the solution to a number of common problems due to their eco-friendly features. To expand their applications, the gelation of ionic liquids has been achieved by using amino acid-based low-molecular-weight compounds. Variation of individual segments in the molecular skeleton of the gelators, which comprise the amino acid and the protecting groups at the N and C termini, led to an understanding of the structure–property correlation of the ionogelation process.

An aromatic ring containing amino acid-based molecules protected with a phenyl or cyclohexyl group at the N terminus were efficient in the gelation of ionic liquids. In the case of aliphatic amino acids, gelation was more prominent with a phenyl group as the N-terminal protecting agent. The probable factors responsible for this supra-molecular association of the gelators in ionic liquids have been studied with the help of field-emission SEM,

<sup>1</sup>H NMR, FTIR, and luminescence studies. It is the hydrophilic–lipophilic balance that needs to be optimized for a molecule to induce gelation of the green solvents. Interestingly, to maximize the benefits from using these green solvents, these ionogels have been employed as templates for the synthesis of uniform-sized TiO<sub>2</sub> nanoparticles (25–30 nm). Furthermore, as a complement to their applications, ionogels serve as efficient adsorbents of both cationic and anionic dyes and were distinctly better relative to their organogel counterparts.

**Keywords:** gels • green chemistry • hydrogen bonds • ionic liquids • nanoparticles

## Introduction

“Ionogels”, as they have been termed on the basis of their imbibing ability of ionic liquids (ILs), have not been subjected to extensive study and are a rather emerging area of interest among scientists.<sup>[1]</sup> ILs have been a revelation as an alternative to toxic and hazardous organic solvents<sup>[2]</sup> and are known as “green solvents” owing to characteristics, such as low vapor pressure, nonvolatility, high thermal stability, nonflammable character, and eco-friendly nature. Investigations that utilize ILs are progressively improving from synthetic chemistry to materials science.<sup>[2,3]</sup> To add to the properties and applications of ILs, efforts have been initiated to immobilize and confine them by using external materials.<sup>[1]</sup>

Néouze et al. showed the confinement of ILs by using an inorganic matrix as in silica-derived networks.<sup>[1h]</sup> Similar confinements were described by Carlin and Fuller by using polymeric organic materials.<sup>[1i]</sup>

Until now, small molecules and polymers were extensively designed to gelate water and/or other organic solvents.<sup>[4]</sup> However, the gelation of ILs with low-molecular-weight gelators (LMWGs) has not grown as rapidly, and there are only a few examples.<sup>[1a–d]</sup> The gelation of ILs with polymeric or nonpolymeric compounds has been termed the ‘quasi-solidification of ionic liquids’.<sup>[1a]</sup> The self-assembly of low-molecular-weight compounds in ILs would obviously add a new dimension to the properties and applications of these green solvents. To this end, Kimizuka and Nakashima succeeded in the formation of ‘glycolipid bilayer membranes’ in ILs.<sup>[1b]</sup> In a few cases, ionogels have been exploited in the development of technological devices, such as dye-sensitized solar cells, and in the synthesis of anisotropic gold nanoparticles.<sup>[1d,5]</sup> However, attempts toward the rational design of LMWGs for ILs are scarce. This is probably attributed to the poor understanding of the self-assembly mechanism during ionogelation, which involves noncovalent interactions

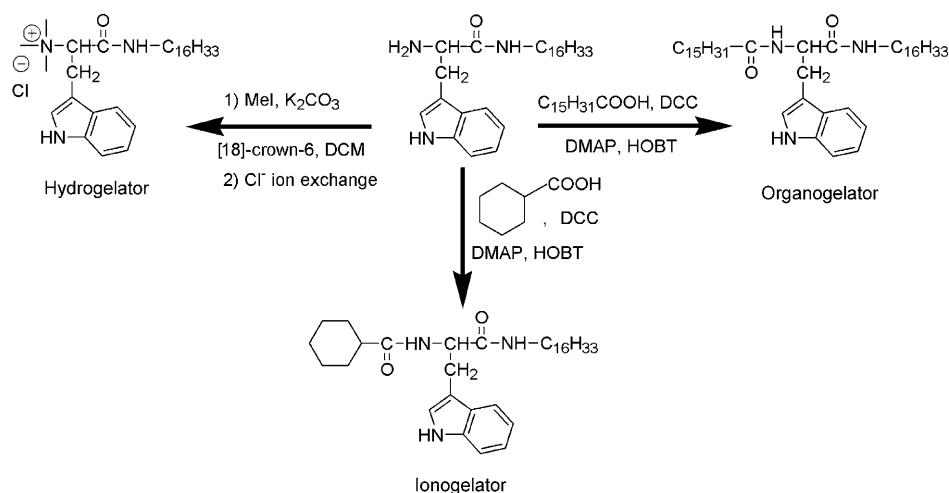
[a] S. Dutta, D. Das, A. Dasgupta, Dr. P. K. Das  
Department of Biological Chemistry  
Indian Association for the Cultivation of Science  
Jadavpur, Kolkata 700032 (India)  
Fax: (+91) 33-24732805  
E-mail: bcpkd@iacs.res.in

Supporting information for this article is available on the WWW under <http://dx.doi.org/10.1002/chem.200901917>.

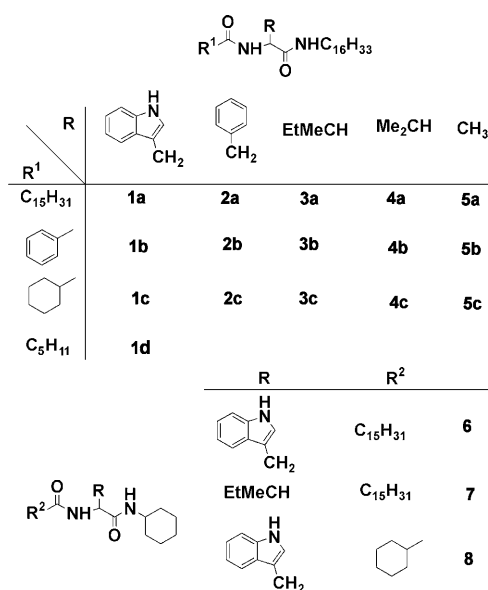
such as electrostatic, van der Waals, and hydrogen bonding. Similar to other gelation processes, an optimized balance between hydrophilicity and lipophilicity is expected to play a crucial role in ionogelation.<sup>[4d,e,6]</sup>

Over the last few years, we have attempted to establish a rationale behind the synthesis of hydro- and organogelators that comprise simple amino acids/dipeptides as basic building blocks through a possible structure–property relationship.<sup>[4d,e,6,7]</sup> The amino acid/dipeptide moiety at the head of an amphiphilic molecule with a long hydrophobic chain at the C terminus and a free amine group at the N terminus is an excellent precursor for the preparation of both organo- and hydrogelators.<sup>[4d,e,6c]</sup> Quaternization of this amine with methyl iodide followed by ion exchange with chloride ions yielded an excellent hydrogelator, whereas coupling of the same amine with a long-chain acid resulted in an efficient organogelator (Scheme 1).<sup>[4d,e,6c]</sup> Interestingly, tuning the counterion of the quaternized amphiphile led to an efficient conversion of a nongelator into a gelator.<sup>[8]</sup> At this point, it would be fascinating if the same precursor amine (Scheme 1) could be converted into an ionogelator by judicious modification in its structure.

ILs generally comprise an organic cation and inorganic anion, a combination that enhances the potential of this type of solvent because one can always modulate either of the two ions to extract a desirable property from the system.<sup>[9]</sup> Keeping in mind that ILs are more hydrophilic than organic solvents, we introduced a phenyl ring at the N terminus of the amine to retain a critical balance. This fine-tuning of the L-tryptophan-based amine led to a molecule with limited ionogelation ability (Scheme 2, Table 1) and further motivated us to introduce a more hydrophobic moiety, that is, a cyclohexyl group at the N terminus of the amine group. This change resulted in the development of an efficient ionogelator (Scheme 2) capable of entrapping a wide range of ILs (Scheme 3). The gelation results, obtained by varying the amino acids and the protecting groups at the N and C termini, helped us to establish a logical structure–



Scheme 1. Synthesis of the hydrogelator, organogelator, and ionogelator from same precursor amine.



Scheme 2. Structure of the compounds.

property correlation. These ionogels showed remarkable dye-adsorption efficiencies from water, which were significantly better than those of the analogous organogels. The synthesis of inorganic metal oxide nanoparticles has been a focus of research owing to their catalytic efficiency and unique optoelectronic properties.<sup>[10]</sup> Ionogel **1c** (Scheme 2) was used as a template to synthesize uniform- and small-sized TiO<sub>2</sub> nanoparticles.

## Results and Discussion

Gelation is a process in which the immobilization of solvents has led to the formation of soft materials with diverse applications that range from advanced materials to biomedicines.<sup>[4,11–13]</sup> It is now quite well established that supramolecular

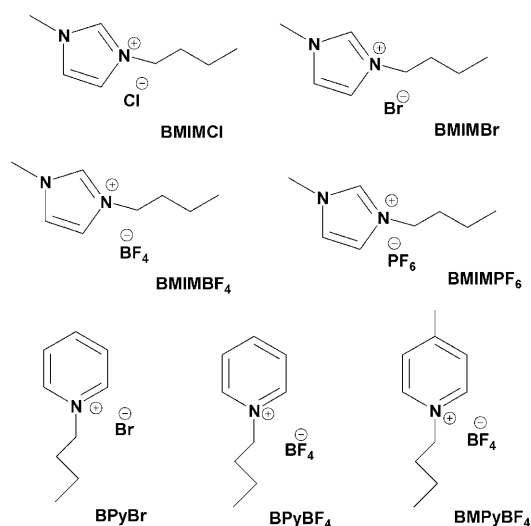
gels formed by the self-assembly of LMWGs either in water or organic solvents is due to an optimized balance of several noncovalent interactions.<sup>[4,6,11]</sup> However, understanding the structure–property correlations of small-molecule ionogelators and their self-assembly mechanism is still in its infancy.

Recently, we designed and developed very efficient hydro- and organogelators with minimum gelation concentrations (MGC) of 0.3 and 0.15 % (w/v), respectively, by using a simple amino acid as the basic scaffold.<sup>[4d,e,6c]</sup> Both

Table 1. Gelation properties of **1–8** in ionic liquids.<sup>[a]</sup>

Compound	BMIMBr (10% aq)	BMIMCl (10% aq)	BMIMBF <sub>4</sub>	BMIMPF <sub>6</sub>	BPyBr (10% aq)	BPyBF <sub>4</sub>	BMPyBF <sub>4</sub>
<b>1a</b>	ins	ins	ins	ins	ins	ins	ins
<b>1b</b>	sol	sol	4.5 (og)	sol	sol	sol	sol
<b>1c</b>	1.3	2.1	1.5 (tg)	2.0 (og)	1.8	1.7	1.7
<b>2a</b>	ins	ins	ins	ins	ins	ins	ins
<b>2b</b>	3.8 (tg)	2.3	1.3	3.1 (og)	2.2	3.5 (og)	4.3 (og)
<b>2c</b>	2.2	2.5	1.5	3.5 (og)	2.6	4.0 (tg)	5.1 (tg)
<b>3a</b>	ins	ins	sol	sol	ins	ins	ins
<b>3b</b>	4.6	2.5	3.1	sol	3.3	4.0 (og)	4.3 (og)
<b>3c</b>	3.6	4.2	3.9	ins	3.6	4.9	4.7 (og)
<b>4a</b>	sol	sol	sol	sol	sol	sol	sol
<b>4b</b>	7.2	7.5	8.0	ins	8.2	sol	7.2
<b>4c</b>	10.0	8.5	9.5 (tg)	ins	9.6	sol	7.1
<b>5a</b>	sol	sol	sol	sol	sol	sol	sol
<b>5b</b>	ins	sol	sol	sol	sol	sol	sol
<b>5c</b>	ins	sol	ins	ins	ins	ins	ins
<b>6</b>	3.1	3.0	2.6	3.5 (og)	3.5	3.2	3.7
<b>7</b>	sol	sol	sol	sol	sol	sol	sol
<b>8</b>	sol	sol	sol	ins	sol	ins	sol

[a] tg = Translucent gel, og = opaque gel, sol = soluble, ins = insoluble, concentration in % w/v.



Scheme 3. Structure of the ionic liquids.

the gelators were synthesized in single steps by two completely different types of modification of a nongelating precursor amine of an amino acid (e.g., L-tryptophan) with a long hydrophobic chain at the C terminus (Scheme 1). Herein, our prime objective was to develop efficient ionogelators in a single step from the same scaffold so that this amine can be considered to be a general precursor for the preparation of any variety of gelators. Initially, we decided to synthesize ionogelators from the precursor amine of L-tryptophan (Scheme 2) and tested the gelation efficiency in different ILs comprising the 1-butyl-3-methylimidazolium (BMIM) moiety and in 1-butylpyridinium (BPy) salts (Scheme 3). Because BMIMBr, BMIMCl, and BPyBr are solids at room temperature, we used 10% water with these ILs (IL/H<sub>2</sub>O = 9:1 w/w) so that the mixture would be a free-flowing liquid.

We introduced a long hydrophobic chain (C<sub>16</sub>) at the N terminus (Scheme 2) as previously reported for organogelators.<sup>[4d]</sup> Protecting groups both at the C and N termini were connected through an amide linkage to the central scaffold. The L-tryptophan-based compound with two long hydrophobic chains at the N and C termini (**1a**) was insoluble in most of the ILs and did not exhibit any gelation ability. Instead this compound gelled the organic solvent toluene (MGC = 1.8% w/v). Considering that ILs are, on the whole, more hydrophilic than organic solvents, we decided to improve the hydrophilicity by incorporating a phenyl ring instead of a long hydrophobic chain at the N terminus (Scheme 2). The resultant molecule **1b** could only gelate BMIMBF<sub>4</sub> at a high MGC value (4.5% w/v). To expand the scope of gelation in different ILs and to judiciously alter the balance between hydrophilicity and hydrophobicity, we introduced a nonplanar cyclohexyl moiety at the N terminus instead of the phenyl ring. The other reason for introducing the cyclohexane ring is because it sometimes facilitates intermolecular hydrogen bonding by positioning itself perpendicular to the amide group.<sup>[4h,11a,14]</sup>

The resultant molecule **1c** exhibited a marked improvement (i.e., threefold) in the gelation of BMIMBF<sub>4</sub> (MGC = 1.5% w/v) relative to **1b** and also showed either a comparable or better gelation ability in other ILs, such as BMIMBr, BMIMCl, and BPyBr with 10% water (Table 1). Interestingly, **1c** also showed gelation ability in different organic solvents (toluene, hexane, CCl<sub>4</sub>, and ethyl acetate) with a MGC of 1.0–2.5% w/v (see Table S1 in the Supporting Information).

As a first step, structural variation was carried out at the central scaffold by changing the L-amino acid moieties with nonpolar aliphatic/aromatic residues to obtain a structure–property correlation for the ionogelators. For each amino acid residue, the protecting group at the N terminus was varied with *n*-hexadecyl, phenyl, and cyclohexyl moieties as carried out for the L-tryptophan-based molecules (**1a–c**; Scheme 2). In the case of all the other amino acid groups used in the present study (L-phenylalanine, L-isoleucine, L-valine, and L-alanine) as the central unit, no ionogelation was observed for the compounds with long-chain protection (i.e., *n*-hexadecyl) at the N terminus (**2a–5a**). However, when L-tryptophan was replaced by L-phenylalanine, (i.e., from **1b** to **2b**), gelation ability was observed in all the ILs (Table 1). Also, the phenyl- and cyclohexyl-substituted compounds (**2b** and **2c**, respectively) exhibited almost comparable gelation efficiencies in varying ILs (Table 1); however,

**2c** always had higher MGC values relative to **1c**, except in BMIMBF<sub>4</sub>, in which both **2b** and **2c** showed similar gelation efficiencies. Interestingly, **2b** not only gelled all the ILs but also showed more than a threefold improvement in gelation efficiency in BMIMBF<sub>4</sub> relative to **1b** (Table 1). The superior ionogelation efficiencies of **1c** and **2b** relative to those of **2c** and **1b**, respectively, might be due to the differences in the hydrophilic–lipophilic balance (HLB) of the gelators. This contrasting gelation behavior could be explained by the difference in the hydrophathy index of the two aromatic amino acid residues.<sup>[4e]</sup> The hydrophathy index represents the relative hydrophilic and hydrophobic properties of the side chain of the amino acid residues.<sup>[15]</sup> Hydrophobic amino acids have larger hydrophathy indices. Despite the presence of aromatic rings in L-phenylalanine and L-tryptophan, these amino acids have contrasting HLBs, as L-phenylalanine has a positive hydrophathy number of 2.8, whereas L-tryptophan has a negative value of –0.9.<sup>[15]</sup> Thus, L-phenylalanine is more hydrophobic, whereas an extended indole ring containing a hydrophilic –NH group imparts additional hydrophilicity to L-tryptophan. Aromatic rings are also an important factor in all forms of gelation because they impart additional  $\pi$ – $\pi$  stacking interactions that facilitate the formation of self-assembly. Thus, it can be inferred that the presence of an extended aromatic residue of L-tryptophan and a cyclohexyl moiety maintained the appropriate HLB for **1c**, thus leading to efficient ionogelation. At this point, it is worth mentioning that the linear chain analogue of the cyclohexyl moiety, that is, a *n*-hexyl-protected N terminus of **1** (**1d**), did not exhibit any ionogelation. On the other hand, the presence of two phenyl rings in **2b** suitably retained the HLB for ionogelation contrary to **1b**, with one indole moiety and a phenyl ring.

The replacement of aromatic amino acids by aliphatic residues clarified the importance of aromatic rings in ionogelation. In the case of L-isoleucine (**3**) and L-valine (**4**), the phenyl ring at the N terminus (i.e., **3b** and **4b**) induced superior ionogelation efficiency relative to the analogous non-aromatic cyclohexyl-substituted gelators **3c** and **4c**. For example, in the case of BMIMCl and water (9:1 w/w), the MGC value of **3b** was 2.5% w/v, which increased to MGC = 4.2% w/v on replacement of the phenyl ring by a cyclohexyl group in **3c**. A similar trend was observed for **4b** and **4c** (Table 1). It seems in the case of nonpolar aliphatic amino acids, substitution of aliphatic cyclohexyl moiety at the N terminus decreases the ionogelation ability because of its overall hydrophobic nature. To be precise, for an aliphatic amino acid, the presence of a phenyl group at the N terminus facilitates the self-assembling process, thus leading to improvement in ionogelation. Intriguingly, **3c** also showed gelation ability in different organic solvents with a MGC of 1.6–2.9% w/v (see Table S1 in the Supporting Information). In accordance with the observed trend, none of the L-alanine-based compounds **5a–c** were ionogelators, possibly because they could not retain the requisite HLB necessary for gelation. Interestingly, the ionogelation efficiency for the aliphatic amino acid-based compounds markedly decreased

with the concurrent steady decrease in the size of the side-chain substitution from **3** (L-isoleucine) to **5** (L-alanine) irrespective of the nature of the protecting group at the N terminus (Table 1).

So far we had tested the gelation efficiency of amino acid-based compounds with a long hydrophobic chain at the C terminus and different protecting groups at the N terminus. We were curious to further investigate whether the ionogelating ability would be affected if the position of the protecting groups was swapped between the termini. To find out the importance of the specificity of the position of the long chain and the phenyl/cyclohexyl group in ionogelation, protecting groups between the C and N termini of **1c** and **3c** were exchanged to prepare **6** and **7**, respectively (Scheme 2). Compounds **1c** and **3c** were chosen to reverse the termini as they were the most efficient ionogelators that contained amino acid residues substituted with aromatic and aliphatic side chains, respectively. The L-tryptophan-based compound **6** with a cyclohexyl-protected C terminus showed moderate gelation efficiency in all the ILs with a MGC of 2.6–3.7% w/v (Table 1). But the gelation ability decreased almost by 1.5–2.5-fold relative to **1c**. In the case of the L-isoleucine analogue **7**, there was no gelation at all of any IL. Thus, swapping the protecting groups between the termini did not improve the ionogelation efficiency. Even incorporation of two cyclohexyl groups at both C and N termini of L-tryptophan (i.e., **8**) did not succeed in gelating the ILs. So, the presence of the long chain at the C terminus of the amino acid is almost indispensable for displaying gelation ability. On the whole, we found that aromatic-ring-containing amino acid-based molecules protected with a phenyl or cyclohexyl group at the N terminus were efficient in ionogelation. Hence, an optimum HLB is needed for a specific molecule to induce gelation of the green solvents. Similarly, in the case of aliphatic amino acids, such as L-isoleucine and L-valine, the gelation was more prominent with a phenyl group as the N-terminal protecting agent.

In the case of ILs that are solid at room temperature, that is, BMIMBr, BMIMCl, and BPyBr, we tested the gelation of the molecules in the presence of 10% water. Thus, this free-flowing medium is a mixture of water and hydrophilic IL. To expand the scope of gelation in only IL-based systems, we decided to replace the water with a hydrophilic IL that is liquid at room temperature. We tested the gelation efficiencies of **1c** and **3c** in a mixture the hydrophilic ILs BMIMBr (solid at room temperature) and BMIMBF<sub>4</sub> in an equal ratio (1:1 w/w). Encouragingly, in this hydrophilic IL mixture both **1c** and **3c** showed comparable or better gelation efficiencies (MGC = 1.2 and 3.2% w/v for **1c** and **3c**, respectively; see Table S1 in the Supporting Information) than with only BMIMBF<sub>4</sub> and BMIMBr in 10% water (Table 1).

**Gel-to-sol transition:** The gelators were dissolved in the desired IL either by heating or irradiating the gelator/IL mixture in a microwave oven at 320 W for 5–10 s. The mixture was left to stand for 30 min, left to cool at room temperature, and checked to see whether they were “stable to inver-

sion" (Figure 1). All the ionogels were thermoreversible in nature, thus they melted upon heating and turned into a gel on cooling, which indicates the self-assembled aggregation of the small molecules in the ILs. The system is at thermo-

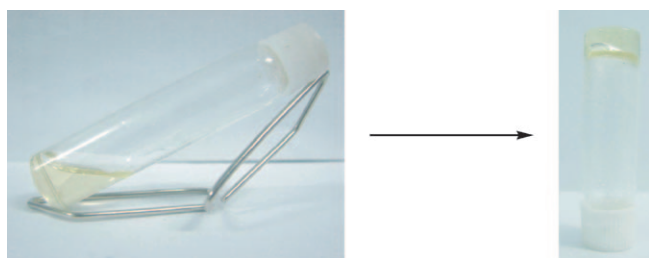


Figure 1. Gelation of **1c** in BPyBF<sub>4</sub> before (left) and after the formation of the ionogel (right).

dynamic equilibrium and there is no kinetic control of the process. The temperature at which this gel-to-sol transition takes place is known as the gel-melting temperature  $T_{\text{gel}}$ , which increases with an increase in the concentration of the gelator molecules (Figure 2).<sup>[7,16]</sup> Interestingly, these ionogels

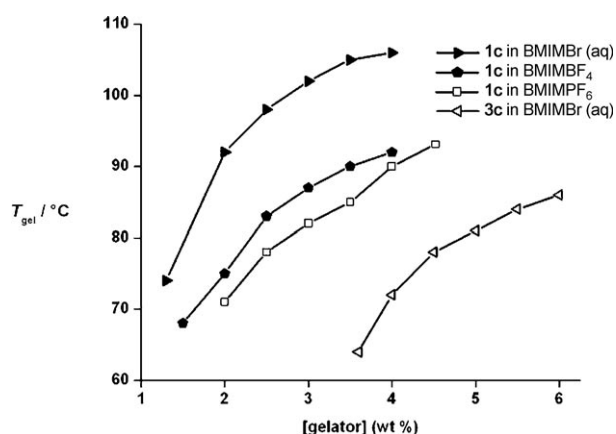


Figure 2. Variation of the gel-to sol transition temperature  $T_{\text{gel}}$  with the gelator concentrations of representative ionogels.

are distinctly high-melting gels relative to the reported hydrogels and organogels. A striking difference was observed in the case of **1c**, in which  $T_{\text{gel}}=74^{\circ}\text{C}$  at MGC=1.3% w/v in BMIMBr (with 10% water), whereas the same compound in toluene gave  $T_{\text{gel}}=48^{\circ}\text{C}$  at MGC=1.0% w/v. Even at a MGC value of 3.5% w/v (a 3.5-fold increase),  $T_{\text{gel}}=70$  and  $103^{\circ}\text{C}$  in toluene and BMIMBr, respectively (Figure 2). Similarly, for other ionogels, the  $T_{\text{gel}}$  value is relatively higher, and in accordance with the gelation efficiency  $T_{\text{gel}}$  is always higher for **1c** than for **3c**.

**Differential scanning calorimetry (DSC):** This technique is important in determining the phase change of a system.<sup>[17]</sup> One can follow the temperature at which a specific change in the system takes place. We take **1c** as a representative ex-

ample because it is the best ionogelator in the present study. A prominent endothermic peak was visible for ionogel **1c** in BMIMBr (Figure 3) at MGC=1.3% w/v. Very interestingly, the temperature ( $72.8^{\circ}\text{C}$ ) at which this peak is present is

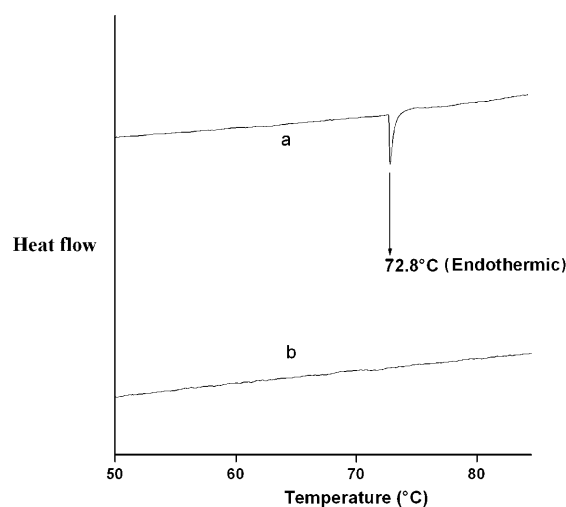


Figure 3. DSC thermograph of a) **1c** in BMIMBr (ionogel) and b) only the ionic liquid.

comparable with  $T_{\text{gel}}=74^{\circ}\text{C}$ , as found in the gel-to-sol transition study. The visually observed gel-to-sol transition at  $T_{\text{gel}}$  corroborates to the temperature found experimentally from the DSC study. In a control experiment with aqueous BMIMBr solution (10% water) without the gelator, no peak was observed in the same temperature range. The heat flow throughout the scan was uniform, thus indicating no phase transition in the absence of a gelator.

**Microscopy studies:** Field-emission scanning electron microscopy (FESEM) was utilized to obtain primary information as to the cause of this self-aggregation at a supramolecular level. The extent of supramolecular aggregation in the IL-based systems was concurrent with the gelation efficiencies of the molecules. Fibrous networks were visible in the microscopy images of the ionogels of **1c** and **3c** (taken as representatives) in BMIMBr (Figure 4a,b). In the case of **1c**, thicker fibrils of approximately 300 nm were observed relative to the fibers of approximately 100 nm for **3c**. The extended aromatic system of the L-tryptophan moiety and the hydrogen-bonding ability of **1c** possibly facilitated the supramolecular association of the fibrils into thicker fibers. On the other hand, the ionogel of **3c** in BMIMBr showed thinner fibers of approximately 100 nm. The absence of an aromatic system might be the cause of this loosely packed supramolecular structure, which was consistent with its comparatively poor ionogelation ability.

Bright field microscopy images of **1c** and **3c** in aqueous BMIMBr solution (10% water) also showed fibrous intertwined networks (Figure 4c,d), which were concurrent with the FESEM images. The pattern of supramolecular aggregation was similar for both molecules in bright field microscop-

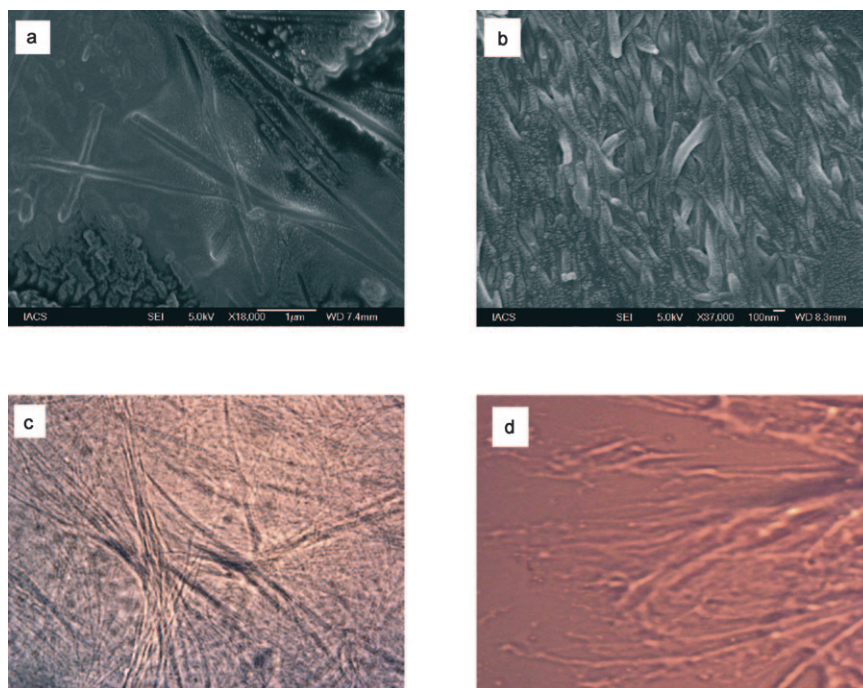


Figure 4. SEM images of a) **1c** in BMIMBr (10% water) and b) **3c** in BMIMBr (10% water), and bright-field microscopy images of c) **1c** in aqueous BMIMBr and d) **3c** in aqueous BMIMBr.

py as well as FESEM images. The self-aggregation of small molecules in ILs thus proceeds through a probable fibrous supramolecular structure.

**<sup>1</sup>H NMR experiments:** <sup>1</sup>H NMR spectroscopic analysis is a powerful tool to investigate the involvement of hydrogen bonding during the process of self-assembled gelation. The protons involved directly in gelation suffer notable shifts when investigated in an immobilized state.<sup>[4c,18]</sup> In this context, we monitored the change in the chemical shift of the amide proton that plays key role in the hydrogen-bonding interactions. Obviously, because of its superior ionogelation efficiency among the others, **1c** was chosen for this study. In deuterated dimethyl sulfoxide ([D<sub>6</sub>]DMSO), that is, in the sol state of **1c**, the amide proton at the N terminus of the L-tryptophan moiety appeared at  $\delta = 5.56$  ppm (Figure 5). With an increase in the BMIMBr content in the medium, a downfield shift of the amide proton was observed. Even at concentration of 10% IL (90% [D<sub>6</sub>]DMSO), the amide proton was notably deshielded ( $\delta = 5.83$  ppm). A consequent increase in IL shifted the proton signal further downfield. In a composition of IL and [D<sub>6</sub>]DMSO of 40:60 (v/v), the chemical shift was shifted as much as up to  $\delta = 6.25$  ppm. Also with an increase in the amount of IL, the nature of the peak became broader and the splitting disappeared. As the amount of IL was increased, a gelation process is induced that obviously involves the molecule concerned. The amide proton, or the whole molecule that was in solution in [D<sub>6</sub>]DMSO, is drawn into a supramolecular association in the presence of the IL. Thus, the spinning nuclei cannot produce individual sharp and strong signals as in the nongelated

state.<sup>[4d,6c,7a,19]</sup> The molecules participating in gelation are merely observable on the NMR timescale due to the large correlation time of the assemblies, which results in a very short transversal relaxation time and produces a broad signal.<sup>[18h]</sup> At the onset of this aggregation mechanism in IL-based systems, there is an obvious participation of the amide group in hydrogen bonding. The amide proton interacts with the neighboring carbonyl group through C=O...H-N hydrogen bonding, which deshields the proton and allows the downfield shift to be observed.<sup>[6c,18e-g]</sup> In this context, we must say that the other protons of the gelator molecule, such as the chiral proton that appears at  $\delta =$

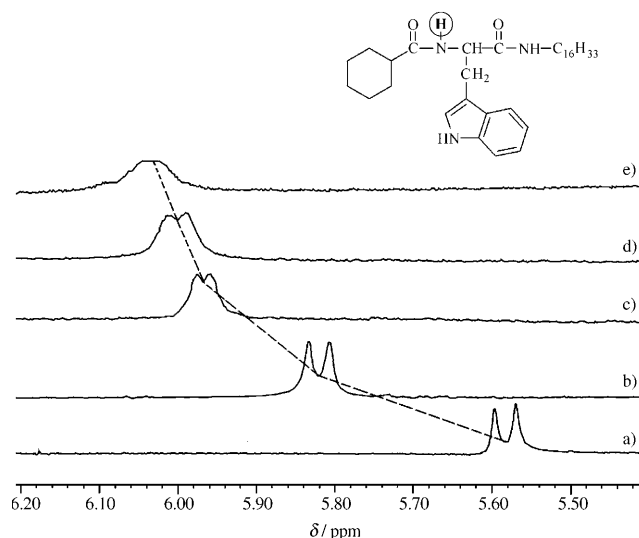


Figure 5. Changes in the amide proton of **1c** with increasing concentration of ionic liquid; **1c** in IL/[D<sub>6</sub>]DMSO at ratios (v/v) of a) 0:100, b) 10:90, c) 20:80, d) 30:70, e) 40:60.

4.44 ppm in [D<sub>6</sub>]DMSO, did not show any significant shifts with an increase in IL concentration. Also the cyclohexyl proton, which appears at  $\delta = 3.00$  ppm, remains more or less constant with varying concentrations of IL. This finding gives us the idea that only those protons (amide) involved in hydrogen bonding in the self-assemblies undergo sufficient chemical shifts.

**FTIR spectroscopic analysis:** We performed FTIR spectroscopic experiments with gelator **1c** in a nongelated solution

state in  $\text{CHCl}_3$  and in a gel state in ILs  $\text{BMIMBF}_4$  and  $\text{BMIMBr}$  (in the presence of 10%  $\text{D}_2\text{O}$ ) at their corresponding MGCs (Figure 6). The FTIR spectrum of the compound in  $\text{CHCl}_3$  showed transmission bands at  $\tilde{\nu}=1645$  and

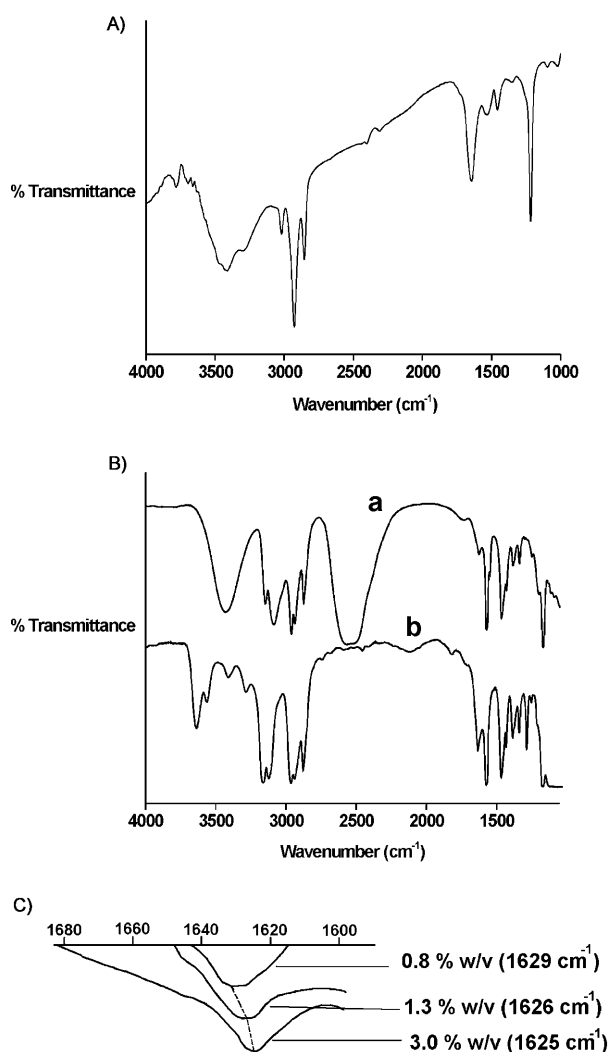


Figure 6. A) FTIR spectra of **1c** in  $\text{CHCl}_3$ , B) Ionogel of **1c** in a) aqueous  $\text{BMIMBr}$  and b)  $\text{BMIMBF}_4$ . C) Shift in the  $\nu(\text{C}=\text{O})$  (amide I) absorption with an increase in the concentration of gelator **1c** in aqueous  $\text{BMIMBr}$ .

$1528\text{ cm}^{-1}$ , which are the characteristic of  $\nu(\text{C}=\text{O})$  (amide I) and  $\delta(\text{N}-\text{H})$  (amide II) frequencies, respectively. A decrease in the  $\nu(\text{C}=\text{O})$  stretching band (amide I) and an increase in the  $\text{N}-\text{H}$  bending band (amide II) was observed in the ionogel state relative to the sol state (Figure 6).<sup>[4d,11b]</sup> The amide I frequency appeared at  $\tilde{\nu}=1634\text{ cm}^{-1}$  for the ionogel in  $\text{BMIMBF}_4$  and at  $\tilde{\nu}=1626\text{ cm}^{-1}$  in  $\text{BMIMBr}$  solution (10%  $\text{D}_2\text{O}$ ). The variations in the decrease in the carbonyl stretching frequencies indicate the probable extent to which this bond is involved in a hydrogen-bonding phenomena with a neighboring amide moiety. Also in concurrence with reported studies, the  $\delta(\text{N}-\text{H})$  (amide II) frequency increased ( $\tilde{\nu} \approx 1570\text{--}1575\text{ cm}^{-1}$ ) for **1c** in the gel of both ILs. We also

tested the concentration-dependent alteration (below MGC to above MGC) in the  $-\text{C}=\text{O}$  stretching frequency of **1c** in aqueous solution of  $\text{BMIMBr}$  (10%  $\text{D}_2\text{O}$ ). The concentrations of **1c** used were 0.8% w/v (below MGC), 1.3% w/v (at MGC), and 3% w/v (above MGC), respectively. The corresponding stretching frequencies were  $\tilde{\nu}=1629$ , 1626, and  $1625\text{ cm}^{-1}$ , respectively (Figure 6C). Thus, by increasing the concentration up to MGC, the intermolecular hydrogen bonding distinctly increased as the frequency of the amide I band decreased. Above MGC, the change in the strength of the hydrogen bonding is obviously negligible as no additional hydrogen bonding was expected to form beyond MGC.<sup>[4d,7]</sup>

**Luminescence study:** The participation of the gelator molecules through hydrophobic interactions during gelation is often investigated by luminescence studies that use any popular hydrophobic probe.<sup>[13c,16,20]</sup> In the present study, we examined the participation of the IL in gelation following the emission spectra of the IL. The luminescence study was performed in  $\text{BMIMBr}$  solution (10%  $\text{H}_2\text{O}$ ) by varying the concentration of gelators **1c** and **3c** (Figure 7). A fluorescence emission was observed at  $\lambda \approx 460\text{ nm}$  when the imida-

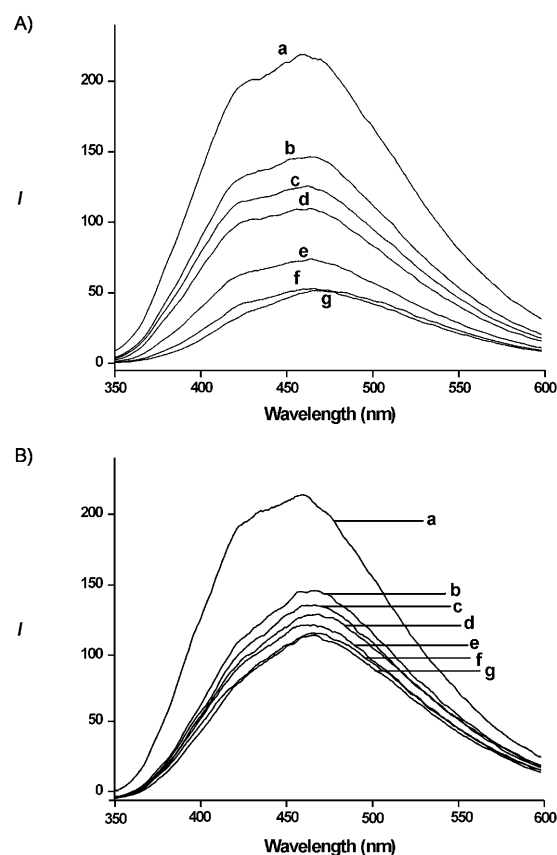


Figure 7. A) Luminescence spectra of a) aqueous  $\text{BMIMBr}$  and the addition of **1c** at concentrations of b) 0.05, c) 0.5, d) 1.0, e) 1.5, f) 2.0, and g) 3.0% w/v. B) Luminescence spectra of a) aqueous  $\text{BMIMBr}$  and the addition of **3c** at concentrations of b) 0.5, c) 1.0, d) 2.0, e) 3.0, f) 4.0, and g) 5.0% w/v.

zolium salt is excited at  $\lambda=320$  nm.<sup>[21]</sup> With a gradual increase in the concentration of the gelator molecule, the emission intensity steadily decreased. At and above the MGC of the gelator, there was almost negligible change in the emission intensity. Without the gelator molecule, the IL molecule remains free, and hence the fluorescence emission was at a maximum intensity. However, with an increase in the concentration of the gelator, the IL becomes immobilized within the self-assembly of the gelator and bound in the supramolecular networks; as a result, the intensity of the fluorescence emission steadily decreased. The excitation wavelength was maintained at  $\lambda=320$  nm to minimize the excitation of the aromatic moiety of the gelator **1c**. As the trend of fluorescence emission was similar for both aromatic and aliphatic side-chain-substituted amino acids (i.e., **1c** and **3c**, respectively), it can be safely concluded that the observed emission is due to the IL. In this context, it was necessary to confirm whether the observed signals were due to fluorescence emission or Raman bands. We carried out an excitation of the pure IL (BMIMBr, 10% H<sub>2</sub>O) from  $\lambda=280$  to 400 nm with intervals of  $\Delta\lambda=10$  nm and recorded the emission peaks simultaneously. Similar experiments were done with the ionogel (**1c** in BMIMBr (2.0% w/v)). In both cases, we found an inconsistent shift in the emission wavelength with highest intensity ( $\lambda_{em}^{max}$ ), which is known to happen in the case of ILs due to the presence of several energetically different associated forms of the imidazolium ions in the IL.<sup>[21a]</sup> However, the possibility of the signal being a Raman band was ruled out as the extent of the shift in the excitation and emission wavelengths was not comparable (no linearity was observed in the plot of  $\lambda_{ex}$  versus  $\lambda_{em}$ ; see Figure S1 in the Supporting Information). Also, the broad nature of the observed bands indicates the absence of a Raman band, which is generally found to be a sharp peak.<sup>[21c]</sup>

**Synthesis of TiO<sub>2</sub> nanoparticles:** The IL-assisted preparation of TiO<sub>2</sub> on the nanoscale level has been studied recently.<sup>[22,23]</sup> However, an ionogel as a template has never been utilized in the synthesis of TiO<sub>2</sub> nanoparticles. Herein, we synthesized TiO<sub>2</sub> nanoparticles by adding titanium tetraisopropoxide to the ionogel of **1c** in aqueous (10% H<sub>2</sub>O) BMIMBr solution and adding an equal amount water fol-

lowed by stirring at room temperature for 48 h. Washing and calcinations of the white material resulted in the formation of a fine white powder. The powder obtained was characterized by using FESEM in which uniform-shaped particles of the dimension of 25–30 nm were observed (Figure 8a). For atomic force microscopy (AFM), the powder was taken in HPLC-grade ethanol and sonicated for 30 min. From this turbid solution, a drop was cast on a silicon wafer and investigated with AFM. TiO<sub>2</sub> nanoparticles of a similar dimension were seen from the AFM image (Figure 8b).

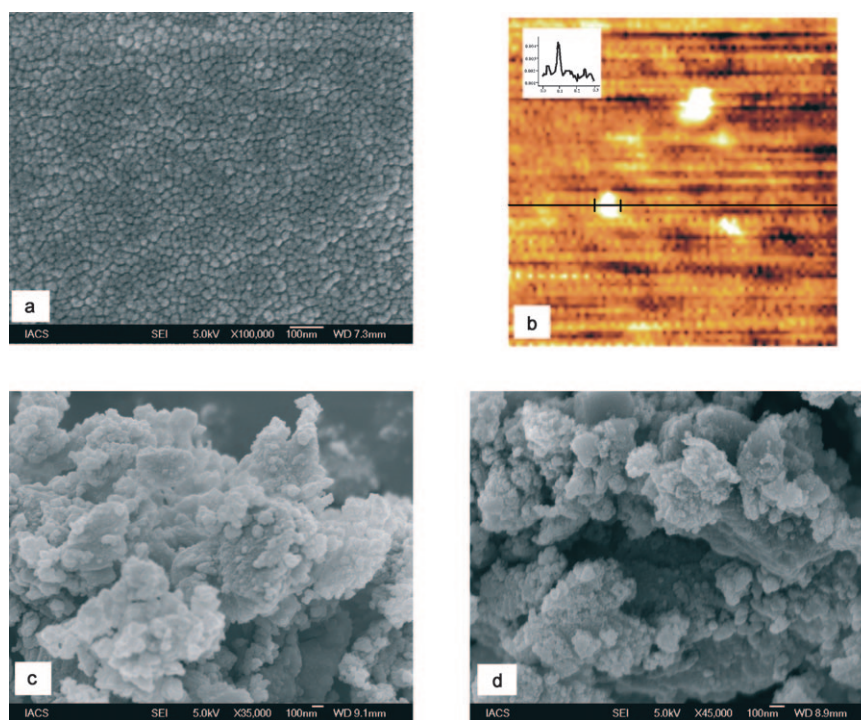


Figure 8. a) FESEM image of TiO<sub>2</sub> prepared in an ionogel; b) AFM image of TiO<sub>2</sub> prepared in an ionogel (inset: cross-sectional analysis along the black line in (b)). FESEM image of TiO<sub>2</sub> prepared in c) an ionic liquid medium and d) with **1c** in BMIMBr below MGC.

However, we were curious to know whether the nanoparticles formed could have different sizes and shapes if a static condition of the experiment was maintained instead of stirring. We repeated the experiment under nonstirring conditions while keeping all the other experimental conditions identical. Similar-sized nanoparticles (25–30 nm) were observed from the FESEM image (see Figure S2 in the Supporting Information). Thus, TiO<sub>2</sub> nanoparticles of comparable size and shape were obtained under both stirring and nonstirring conditions. We believe that diffusion of the particles in the gel template is facilitated under stirring, whereas normal spontaneous diffusion takes place without stirring, thus resulting in similar uniformity of the nanoparticles. However, in the absence of the gelator or at a concentration (0.5% w/v) below the MGC, aggregation of the TiO<sub>2</sub> particles was observed (Figure 8c,d). Hence, the supramolecular gel network of the ionogel at MGC is an important factor in the formation of uniform- and small-sized TiO<sub>2</sub> nanoparti-

cles. The XRD study of the nanoparticle powder showed peaks (Figure 9) that correspond to standard anatase TiO<sub>2</sub> without the formation of any other crystalline product, and the broad peak also indicates the formation of small-sized TiO<sub>2</sub> particles.<sup>[24]</sup>

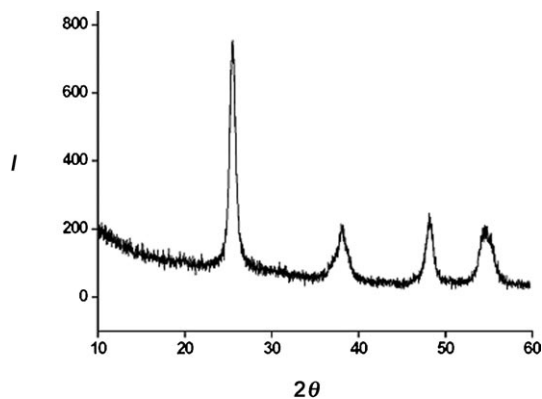


Figure 9. XRD spectra of TiO<sub>2</sub> obtained from an ionogel template (using **1c** in aqueous BMIMBr).

**Dye-adsorption study:** Environmental hazards have looked ominous and it is a growing problem that demands serious attention. Dyes are colored substances that are used hugely in versatile fields, such as the fabric and tanning industries. Removal of these toxic dyes from wastewater has been a matter of concern. Activated charcoal, clay, porcelain, and substances with a high porosity or large surface area have been used for dye removal from wastewater.<sup>[25]</sup> To this end, we previously used xerogels of organogels for efficient dye removal because they comprise both hydrophilic and hydrophobic domains, which could efficiently adsorb the dye.<sup>[4d,e]</sup> Having used ILs as solvents for gelation, we used this ionogel as a dye-adsorbing agent. This time, water-immiscible ionogels of the hydrophobic IL BMIMPF<sub>6</sub> was used. BMIMPF<sub>6</sub> (100 μL) containing gelator **1c** (2.0%, w/v; just after heating in the microwave oven so that it forms a gel) was added to a stock solution (0.01 mM) of crystal violet (cationic) and naphthol blue black (anionic) in water. The neat ionogel descended through the aqueous solution of the dye. A similar method was applied for the organogels (2.0% w/v) of **1c** in toluene. This experiment was carried out to compare the efficiency of the hydrophobic organo- and ionogels. Almost 65% of the cationic dye was adsorbed in the ionogel of **1c** within 5 min, whereas this value for the anionic dye was 45% (Figure 10). More than 90% of the cationic and anionic dyes were removed within 8 and 20 h, respectively, by using the ionogel of **1c**. On the other hand, the organogels removed dyes from the aqueous dye solution at a slower rate because 50% adsorption of dye took almost 6 h for crystal violet and 20 h for naphthol blue black (see Figure S3 in the Supporting Information). Both the cationic (Figure 11) and anionic dyes are adsorbed by the ionogels to a more or less similar extent, which is notably better than

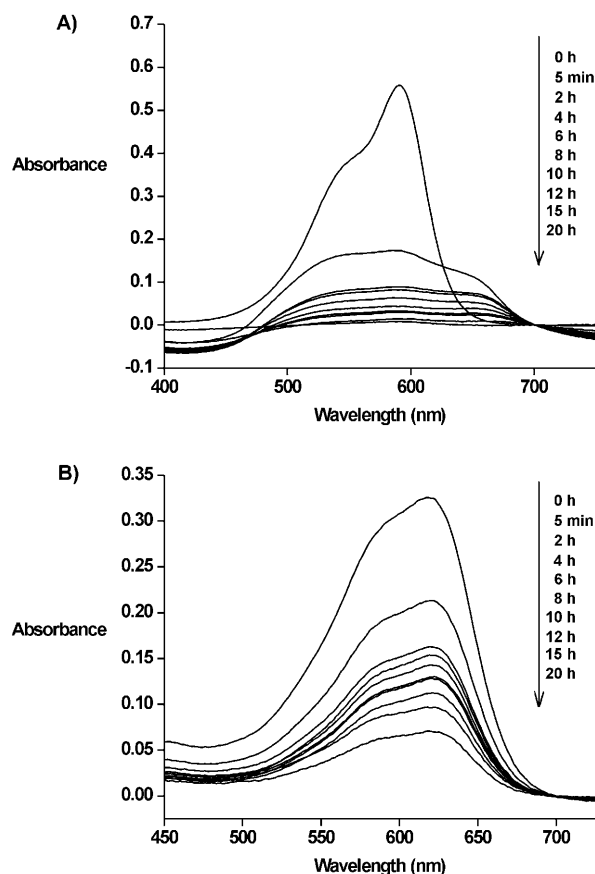


Figure 10. UV/Vis spectroscopic study of the time-dependant removal of crystal violet and naphthol blue black by using an ionogel (**1c** in BMIMPF<sub>6</sub>).

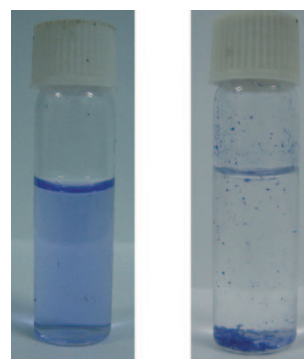


Figure 11. Solution of 0.01 mM of crystal violet before and after treatment of the ionogel (**1c** in BMIMPF<sub>6</sub>).

the analogous organogels. Although BMIMPF<sub>6</sub> is hydrophobic like the organic solvent used (i.e., toluene), the inherent ionic character within the ionogel presumably facilitates the adsorption of the cationic/anionic dyes. A parallel set of control experiments (in the absence of a gelator) was carried out to compare the dye adsorption efficiencies of the neat IL (see Figure S3 in the Supporting Information). The rate of the adsorption of the dyes with the hydrophobic IL was even slower. For crystal violet, 90% of the dye removal

took as long as 30 h, whereas in the presence of a gelator (ionogel) 90% of the dye was removed within 8 h. For naphthol blue black, even after 30 h only about 35% of the dye was removed by the neat IL. However, in the presence of the gelator, 90% of the dye was removed within 12 h. Hence, the supramolecular network of the ionogel in the presence of a gelator might have facilitated the adsorption process. Also, dye adsorption by solid or quasisolid materials is an advantageous process because the residual clean water can be removed easily.

## Conclusions

Herein, the efficient gelation of ILs has been achieved by using low-molecular-weight amino acid-based compounds. Importantly, these ionogelators were prepared from the same precursor scaffold from which hydrogelators and organogelators were obtained. A possible structure–property correlation has been established between the molecule and its ionogelation ability by the systematic variation of the amino acids and protecting groups. In concurrence with the gelation behavior of small molecules in water and organic solvent, a critical HLB is necessary for the formation of the supramolecular association in ILs that would lead to the development of ionogels. The importance of aromaticity was established because in many cases the presence of a phenyl ring either in the amino acid or the protecting group is crucial for the gelation of ILs. The ionogel template was found to have an application in the synthesis of uniform-shaped TiO<sub>2</sub> nanoparticles (25–30 nm). Additionally, these supramolecular aggregates in ILs were exploited in the adsorption of both cationic and anionic dyes from aqueous solution, which exhibited markedly higher dye-adsorption efficiencies relative to those of the analogous organogels. With the growing significance of ILs and the matrices of immobilized ILs, the present work has provided an opportunity to understand the gelation of ILs with an important structural correlation and to exploit them in the synthesis of TiO<sub>2</sub> nanoparticles and wastewater treatment.

## Experimental Section

**General:** All the amino acids, *n*-hexadecyl amine, dicyclohexylcarbodiimide (DCC), 4-*N,N*-(dimethyl)aminopyridine (DMAP), 1-hydroxybenzotriazole (HOBT), benzoic acid, cyclohexane carboxylic acid, cyclohexyl amine, *n*-hexadecanoic acid, and all the solvents were purchased from SRL (India). All the deuterated solvents for the NMR and FTIR spectroscopic experiments and titanium tetraisopropoxide were obtained from the Aldrich Chemical Co. TLC analysis was performed on Merck pre-coated silica gel 60-F<sub>254</sub> plates. The <sup>1</sup>H NMR spectra were recorded on an AVANCE 300 MHz (Bruker) spectrometer. The mass-spectrometric data were acquired by electron spray ionization (ESI) on a Q-TOF-micro quadrupole mass spectrometer (Micromass).

**Synthesis:** The small molecules were prepared by following a standard protocol as done previously.<sup>[44]</sup> Briefly, a *tert*-butyloxycarbonyl (Boc)-protected L-amino acid was coupled with *n*-alkylamine or cyclohexyl amine (for **6–8**) by using DCC (1 equiv) in dry dichloromethane. The pure Boc-

protected amide was obtained through column chromatography on silica gel (60–120 mesh) and ethyl acetate/hexane as the eluent. The product was deprotected with trifluoroacetic acid (TFA; 2 equiv) in dry dichloromethane. After stirring for 2 h, the solvents were removed on a rotary evaporator, and the mixture was dissolved in ethyl acetate. The ethyl acetate portion was thoroughly washed with aqueous 10% sodium carbonate solution followed by brine to neutrality. The organic portion was dried over anhydrous sodium sulfate and concentrated to obtain the corresponding amine. The amine was coupled with the desired acid (palmitic acid/benzoic acid/cyclohexane carboxylic acid) by using DCC (1 equiv) in dry dichloromethane. The purified product was obtained by column chromatography on silica gel (60–120 mesh) and ethyl acetate/toluene as the eluent to yield the purified product.

**1a:** [ $\alpha$ ]<sub>D</sub><sup>20</sup> = −18.2° (*c* = 3.5 in CHCl<sub>3</sub>); <sup>1</sup>H NMR (300 MHz, CDCl<sub>3</sub>, 25°C TMS):  $\delta$  = 8.14 (s, 1H), 7.72–7.65 (d, 1H), 7.34–7.26 (d, 1H), 7.22–7.05 (m, 3H), 5.65 (br, 1H), 5.19 (br, 1H), 4.39–4.37 (m, 1H), 3.28–3.27 (m, 2H), 3.17–3.05 (m, 2H), 2.17–2.15 (m, 2H), 1.90–1.67 (m, 4H), 1.55–1.08 (br, 50H), 0.85–0.92 ppm (m, 6H); ESI-MS: *m/z*: calcd for: 688.7579 [*M*<sup>+</sup>+Na]; found: 665.5859 [*M*<sup>+</sup>]; elemental analysis calcd (%) for C<sub>43</sub>H<sub>75</sub>N<sub>3</sub>O<sub>2</sub>: C 77.54, H 11.35, N 6.31; found: C 77.98, H 11.18, N 6.86.

**1b:** [ $\alpha$ ]<sub>D</sub><sup>20</sup> = −11.2° (*c* = 3.2 in CHCl<sub>3</sub>); <sup>1</sup>H NMR (300 MHz, CDCl<sub>3</sub>, 25°C TMS):  $\delta$  = 8.10–8.08 (br, 1H), 7.31–6.97 (m, 10H), 6.45–6.40 (d, 1H), 6.12–6.05 (d, 1H), 4.63–4.56 (m, 1H), 3.14–3.08 (m, 2H), 2.88–2.84 (t, 2H), 1.58–1.49 (m, 2H), 1.29–1.15 (br, 26H), 0.93–0.85 ppm (t, 3H); ESI-MS: *m/z*: calcd for: 554.2534 [*M*<sup>+</sup>+Na]; found: 531.3825 [*M*<sup>+</sup>]; elemental analysis calcd (%) for C<sub>34</sub>H<sub>49</sub>N<sub>3</sub>O<sub>2</sub>: C 76.79, H 9.29, N 7.90; found: C 77.05, H 9.71, N 7.55.

**1c:** [ $\alpha$ ]<sub>D</sub><sup>20</sup> = −15.0° (*c* = 2.0 in CHCl<sub>3</sub>); <sup>1</sup>H NMR (300 MHz, CDCl<sub>3</sub>, 25°C TMS):  $\delta$  = 8.08 (s, 1H), 7.77–7.75 (d, 1H), 7.38–7.35 (d, 1H), 7.26–7.12 (m, 3H), 6.31–6.29 (d, 1H), 5.51 (br, 1H), 4.70–4.66 (m, 1H), 3.22–3.11 (d, 2H), 3.07–3.05 (t, 2H), 2.12–2.05 (m, 1H), 1.46–1.08 (br, 38H), 0.88–0.86 ppm (t, 3H); ESI-MS: *m/z*: calcd for: 560.1645 [*M*<sup>+</sup>+Na]; found: 537.4294 [*M*<sup>+</sup>]; elemental analysis calcd (%) for C<sub>34</sub>H<sub>55</sub>N<sub>3</sub>O<sub>2</sub>: C 75.93, H 10.31, N 7.81; found: C 75.48, H 10.53, N 8.07.

**1d:** [ $\alpha$ ]<sub>D</sub><sup>20</sup> = −13.2° (*c* = 2.8 in CHCl<sub>3</sub>); <sup>1</sup>H NMR (300 MHz, CDCl<sub>3</sub>, 25°C TMS):  $\delta$  = 8.05 (s, 1H), 7.45–7.35 (d, 1H), 7.26–7.22 (d, 1H), 7.05–7.01 (m, 3H), 5.56 (br, 1H), 5.23 (br, 1H), 4.54–4.48 (m, 1H), 3.19–3.16 (m, 2H), 3.03–2.95 (m, 2H), 2.23–2.20 (m, 2H), 1.88–1.77 (m, 4H), 1.43–1.15 (br, 30H), 0.88–0.96 ppm (m, 6H); ESI-MS: *m/z*: calcd for: 548.2578 [*M*<sup>+</sup>+Na]; found: 525.4294 [*M*<sup>+</sup>]; elemental analysis calcd (%) for C<sub>33</sub>H<sub>55</sub>N<sub>3</sub>O<sub>2</sub>: C 75.38, H 10.54, N 7.99; found: C 75.57, H 10.15, N 8.26.

**2a:** [ $\alpha$ ]<sub>D</sub><sup>20</sup> = −9.0° (*c* = 1.0 in CHCl<sub>3</sub>); <sup>1</sup>H NMR (300 MHz, CDCl<sub>3</sub>, 25°C TMS):  $\delta$  = 7.26–7.21 (m, 5H), 6.75–6.72 (d, 1H), 6.02 (br, 1H), 4.63–4.61 (m, 1H), 3.13–3.01 (m, 2H), 2.97–2.93 (t, 2H), 2.36–2.32 (t, 2H), 2.16–2.03 (m, 2H), 1.63–1.61 (m, 2H), 1.55–1.11 (br, 50H), 0.88 ppm (m, 6H); ESI-MS: *m/z*: calcd for: 649.6364 [*M*<sup>+</sup>+Na]; found: 626.5750 [*M*<sup>+</sup>]; elemental analysis calcd (%) for C<sub>41</sub>H<sub>74</sub>N<sub>2</sub>O<sub>2</sub>: C 78.53, H 11.90, N 4.47; found: C 78.48, H 11.35, N 4.62.

**2b:** [ $\alpha$ ]<sub>D</sub><sup>20</sup> = −11.2° (*c* = 3.4 in CHCl<sub>3</sub>); <sup>1</sup>H NMR (300 MHz, CDCl<sub>3</sub>, 25°C TMS):  $\delta$  = 7.76–7.26 (m, 10H), 6.97–6.94 (d, 1H), 5.69 (br, 1H), 4.80–4.73 (m, 1H), 3.30–3.19 (m, 2H), 3.16–3.03 (m, 2H), 1.41–1.36 (m, 2H), 1.34–1.25 (br, 26H), 0.90–0.85 ppm (t, 3H); ESI-MS: *m/z*: calcd for: 515.3167 [*M*<sup>+</sup>+Na]; found: 492.3716 [*M*<sup>+</sup>]; elemental analysis calcd (%) for C<sub>32</sub>H<sub>48</sub>N<sub>2</sub>O<sub>2</sub>: C 78.00, H 9.82, N 5.69; found: C 77.62, H 9.68, N 5.58.

**2c:** [ $\alpha$ ]<sub>D</sub><sup>20</sup> = −10.3° (*c* = 4.1 in CHCl<sub>3</sub>); <sup>1</sup>H NMR (300 MHz, CDCl<sub>3</sub>, 25°C TMS):  $\delta$  = 7.7–7.44 (m, 5H), 6.42–6.39 (d, 1H), 5.80 (s, 1H), 4.62–4.55 (m, 1H), 3.22–3.11 (m, 2H), 3.09–2.98 (m, 2H), 2.37–2.31 (m, 1H), 1.56–1.58 (m, 2H), 1.53–1.15 (br, 36 H), 0.88–0.86 ppm (t, 3H); ESI-MS: *m/z*: calcd for: 521.4594 [*M*<sup>+</sup>+Na]; found: 498.4185 [*M*<sup>+</sup>]; elemental analysis calcd (%) for C<sub>32</sub>H<sub>54</sub>N<sub>2</sub>O<sub>2</sub>: C 77.06, H 10.91, N 5.62; found: C 77.33, H 10.58, N 5.85.

**3a:** [ $\alpha$ ]<sub>D</sub><sup>20</sup> = −9.5° (*c* = 2.1 in CHCl<sub>3</sub>); <sup>1</sup>H NMR (300 MHz, CDCl<sub>3</sub>, 25°C TMS):  $\delta$  = 6.23 (s, 1H), 5.10–5.08 (d, 1H), 4.14–4.09 (m, 1H), 3.44–3.40 (br, 2H), 3.26–3.19 (m, 3H), 1.47–1.43 (br, 4H), 1.35–1.11 (br, 55H), 0.89–0.84 ppm (t, 9H); ESI-MS: *m/z*: calcd for: 615.5254 [*M*<sup>+</sup>+Na]; found: 592.5907 [*M*<sup>+</sup>]; elemental analysis calcd (%) for C<sub>38</sub>H<sub>76</sub>N<sub>2</sub>O<sub>2</sub>: C 76.96, H 12.92, N 4.72; found: C 76.56, H 12.69, N 4.55.

**3b:**  $[\alpha]_{\text{D}}^{20} = -15.7^\circ$  ( $c = 3.1$  in  $\text{CHCl}_3$ );  $^1\text{H NMR}$  (300 MHz,  $\text{CDCl}_3$ ,  $25^\circ\text{C}$  TMS):  $\delta = 7.81\text{--}7.4$  (m, 5H),  $6.98\text{--}6.95$  (d, 1H),  $6.29\text{--}6.27$  (br, 1H),  $4.47\text{--}4.41$  (m, 1H),  $3.48\text{--}3.28$  (m, 2H),  $3.26\text{--}3.15$  (m, 1H),  $1.52\text{--}1.47$  (m, 2H),  $1.25\text{--}1.10$  (br, 28 H),  $0.99\text{--}0.85$  ppm (m, 9H); ESI-MS:  $m/z$ : calcd for:  $481.2701 [M^+ + \text{Na}]$ ; found:  $458.3872 [M^+]$ ; elemental analysis calcd (%) for  $\text{C}_{29}\text{H}_{50}\text{N}_2\text{O}_2$ : C 75.93, H 10.99, N 6.11; found: C 75.68, H 11.05, N 5.87.

**3c:**  $[\alpha]_{\text{D}}^{20} = -7.2^\circ$  ( $c = 3.3$  in  $\text{CHCl}_3$ );  $^1\text{H NMR}$  (300 MHz,  $\text{CDCl}_3$ ,  $25^\circ\text{C}$  TMS):  $\delta = 6.10\text{--}6.08$  (d, 1H),  $5.97$  (m, 1H),  $4.32\text{--}4.15$  (m, 1H),  $3.23$  (br, 2H),  $2.12\text{--}1.82$  (m, 2H),  $1.82\text{--}1.77$  (m, 2H),  $1.25\text{--}1.07$  (br, 38H),  $0.89\text{--}0.91$  ppm (m, 9H); ESI-MS:  $m/z$ : calcd for:  $487.3672 [M^+ + \text{Na}]$ ; found:  $464.4342 [M^+]$ ; elemental analysis calcd (%) for  $\text{C}_{29}\text{H}_{56}\text{N}_2\text{O}_2$ : C 74.94, H 12.14, N 6.03; found: C 74.55, H 11.84, N 6.18.

**4a:**  $[\alpha]_{\text{D}}^{20} = -18.4^\circ$  ( $c = 4.7$  in  $\text{CHCl}_3$ );  $^1\text{H NMR}$  (300 MHz,  $\text{CDCl}_3$ ,  $25^\circ\text{C}$  TMS):  $\delta = 6.27$  (s, 1H),  $5.28\text{--}5.25$  (m, 1H),  $3.83\text{--}3.73$  (m, 1H),  $3.28\text{--}3.19$  (m, 2H),  $2.75$  (m, 1H),  $2.35\text{--}2.20$  (m, 2H),  $2.08\text{--}2.04$  (m, 2H),  $1.64\text{--}1.58$  (m, 2H),  $1.49\text{--}1.11$  (br, 50H),  $0.95\text{--}0.85$  ppm (m, 12H); ESI-MS:  $m/z$ : calcd for:  $601.5382 [M^+ + \text{Na}]$ ; found:  $578.5750 [M^+]$ ; elemental analysis calcd (%) for  $\text{C}_{37}\text{H}_{74}\text{N}_2\text{O}_2$ : C 76.75, H 12.88, N 4.84; found: C 76.55, H 13.01, N 5.08.

**4b:**  $[\alpha]_{\text{D}}^{20} = -10.0^\circ$  ( $c = 6.0$  in  $\text{CHCl}_3$ );  $^1\text{H NMR}$  (300 MHz,  $\text{CDCl}_3$ ,  $25^\circ\text{C}$  TMS):  $\delta = 7.58\text{--}7.43$  (m, 5H),  $6.31$  (br, 1H),  $5.45$  (br, 1H),  $4.63\text{--}4.51$  (m, 1H),  $3.20\text{--}3.15$  (m, 2H),  $2.96\text{--}2.89$  (m, 1H),  $1.57\text{--}1.45$  (br, 2H),  $1.42\text{--}1.19$  (br, 26H),  $0.97\text{--}0.85$  ppm (m, 9H); ESI-MS:  $m/z$ : calcd for:  $467.1724 [M^+ + \text{Na}]$ ; found:  $444.3716 [M^+]$ ; elemental analysis calcd (%) for  $\text{C}_{28}\text{H}_{48}\text{N}_2\text{O}_2$ : C 75.63, H 10.88, N 6.30; found: C 75.32, H 11.11, N 6.44.

**4c:**  $[\alpha]_{\text{D}}^{20} = -10.1^\circ$  ( $c = 4.2$  in  $\text{CHCl}_3$ );  $^1\text{H NMR}$  (300 MHz,  $\text{CDCl}_3$ ,  $25^\circ\text{C}$  TMS):  $\delta = 6.20$  (br, 1H),  $5.27$  (br, 1H),  $3.86\text{--}3.84$  (m, 1H),  $3.26\text{--}3.22$  (t, 2H),  $2.36\text{--}2.29$  (m, 1H),  $2.06\text{--}1.91$  (m, 1H),  $1.74\text{--}1.65$  (m, 2H),  $1.47\text{--}1.25$  (br, 36H),  $0.95\text{--}0.88$  ppm (m, 9H); ESI-MS:  $m/z$ : calcd for:  $473.2529 [M^+ + \text{Na}]$ ; found:  $450.4185 [M^+]$ ; elemental analysis calcd (%) for  $\text{C}_{28}\text{H}_{54}\text{N}_2\text{O}_2$ : C 74.61, H 12.08, N 6.21; found: C 75.01, H 11.88, N 6.07.

**5a:**  $[\alpha]_{\text{D}}^{20} = -14.0^\circ$  ( $c = 5.2$  in  $\text{CHCl}_3$ );  $^1\text{H NMR}$  (300 MHz,  $\text{CDCl}_3$ ,  $25^\circ\text{C}$  TMS):  $\delta = 6.25$  (s, 1H),  $5.56$  (br, 1H),  $3.44\text{--}3.26$  (m, 1H),  $3.24\text{--}3.19$  (m, 2H),  $1.65\text{--}1.58$  (m, 2H),  $1.46\text{--}1.44$  (m, 4H),  $1.30\text{--}1.06$  (m, 53H),  $0.99\text{--}0.87$  ppm (m, 6H); ESI-MS:  $m/z$ : calcd for:  $573.2523 [M^+ + \text{Na}]$ ; found:  $550.5437 [M^+]$ ; elemental analysis calcd (%) for  $\text{C}_{35}\text{H}_{70}\text{N}_2\text{O}_2$ : C 76.30, H 12.81, N 5.08; found: C 76.12, H 12.56, N 5.23.

**5b:**  $[\alpha]_{\text{D}}^{20} = -10.6^\circ$  ( $c = 5.5$  in  $\text{CHCl}_3$ );  $^1\text{H NMR}$  (300 MHz,  $\text{CDCl}_3$ ,  $25^\circ\text{C}$  TMS):  $\delta = 8.10\text{--}7.44$  (m, 5H),  $6.15\text{--}6.12$  (br, 1H),  $4.98$  (br, 1H),  $4.12\text{--}4.07$  (m, 1H),  $3.27\text{--}3.20$  (m, 2H),  $1.48\text{--}1.44$  (m, 2H),  $1.35\text{--}1.25$  (m, 29H),  $0.90\text{--}0.85$  ppm (t, 3H); ESI-MS:  $m/z$ : calcd for:  $439.4571 [M^+ + \text{Na}]$ ; found:  $416.3403 [M^+]$ ; elemental analysis calcd (%) for  $\text{C}_{26}\text{H}_{44}\text{N}_2\text{O}_2$ : C 74.95, H 10.64, N 6.72; found: C 75.18, H 11.03, N 6.93.

**5c:**  $[\alpha]_{\text{D}}^{20} = -15.2^\circ$  ( $c = 3.5$  in  $\text{CHCl}_3$ );  $^1\text{H NMR}$  (300 MHz,  $\text{CDCl}_3$ ,  $25^\circ\text{C}$  TMS):  $\delta = 6.35$  (br, 1H),  $5.42$  (d, 1H),  $3.93\text{--}3.89$  (m, 1H),  $3.24\text{--}3.19$  (m, 2H),  $2.30\text{--}2.25$  (m, 1H),  $1.94\text{--}1.89$  (m, 2H),  $1.76\text{--}1.62$  (m, 7H),  $1.47\text{--}1.23$  (br, 32H),  $0.93\text{--}0.84$  ppm (t, 3H); ESI-MS:  $m/z$ : calcd for:  $445.1452 [M^+ + \text{Na}]$ ; found:  $422.3872 [M^+]$ ; elemental analysis calcd (%) for  $\text{C}_{26}\text{H}_{50}\text{N}_2\text{O}_2$ : C 73.88, H 11.92, N 6.63; found: C 74.06, H 11.72, N 6.98.

**6:**  $[\alpha]_{\text{D}}^{20} = -16.0^\circ$  ( $c = 5.6$  in  $\text{CHCl}_3$ );  $^1\text{H NMR}$  (300 MHz,  $\text{CDCl}_3$ ,  $25^\circ\text{C}$  TMS):  $\delta = 8.11$  (s, 1H),  $7.78\text{--}7.68$  (d, 1H),  $7.37\text{--}7.35$  (d, 1H),  $7.23\text{--}7.05$  (m, 3H),  $6.33\text{--}6.31$  (d, 1H),  $5.45$  (br, 1H),  $4.35$  (br, 1H),  $3.61\text{--}3.48$  (m, 1H),  $3.09\text{--}3.01$  (t, 2H),  $2.21\text{--}2.16$  (t, 2H),  $1.95\text{--}1.91$  (m, 2H),  $1.58\text{--}1.11$  (m, 34 H),  $0.96\text{--}0.85$  ppm (t, 3H); ESI-MS:  $m/z$ : calcd for:  $546.3157 [M^+ + \text{Na}]$ ; found:  $523.4138 [M^+]$ ; elemental analysis calcd (%) for  $\text{C}_{33}\text{H}_{53}\text{N}_3\text{O}_2$ : C 75.67, H 10.20, N 8.02; found: C 75.42, H 10.28, N 8.23.

**7:**  $[\alpha]_{\text{D}}^{20} = -11.7^\circ$  ( $c = 6.2$  in  $\text{CHCl}_3$ );  $^1\text{H NMR}$  (300 MHz,  $\text{CDCl}_3$ ,  $25^\circ\text{C}$  TMS):  $\delta = 6.42\text{--}6.40$  (d, 1H),  $5.51\text{--}5.43$  (br, 1H),  $4.68\text{--}4.66$  (m, 1H),  $3.32\text{--}3.27$  (m, 1H),  $3.15\text{--}3.02$  (m, 1H),  $2.20\text{--}2.15$  (m, 2H),  $1.70\text{--}1.56$  (br, 6H),  $1.52\text{--}1.24$  (br, 35H),  $0.96\text{--}0.87$  ppm (m, 6H); ESI-MS:  $m/z$ : calcd for:  $473.4743 [M^+ + \text{Na}]$ ; found:  $450.4185 [M^+]$ ; elemental analysis calcd (%) for  $\text{C}_{28}\text{H}_{54}\text{N}_2\text{O}_2$ : C 74.61, H 12.08, N 6.21; found: C 74.47, H 11.87, N 6.09.

**8:**  $[\alpha]_{\text{D}}^{20} = -21.2^\circ$  ( $c = 5.7$  in  $\text{CHCl}_3$ );  $^1\text{H NMR}$  (300 MHz,  $\text{CDCl}_3$ ,  $25^\circ\text{C}$  TMS):  $\delta = 8.09$  (s, 1H),  $7.70\text{--}7.68$  (d, 1H),  $7.37\text{--}7.35$  (d, 1H),  $7.20\text{--}7.05$  (m, 3H),  $6.35$  (br, 1H),  $5.44$  (br, 1H),  $4.65$  (m, 1H),  $3.61\text{--}3.48$  (m, 1H),

$3.15\text{--}3.08$  (t, 2H),  $2.04\text{--}1.95$  (m, 1H),  $1.50\text{--}1.37$  (m, 8H),  $1.25\text{--}0.88$  ppm (m, 12H); ESI-MS: calcd for:  $418.1471 [M^+ + \text{Na}]$ ; found:  $395.2573 [M^+]$ ; elemental analysis calcd (%) for  $\text{C}_{22}\text{H}_{33}\text{N}_3\text{O}_2$ : C 72.88, H 8.41, N 10.62; found: C 72.52, H 8.59, N 10.71.

**Synthesis of ILs:** The ILs were prepared by following a standard protocol.<sup>[2f,26]</sup> Briefly, BMIMBr, BMIMCl, and BPyBr were obtained through a microwave-assisted synthesis, after which they were washed with dry diethyl ether and ethyl acetate. The corresponding tetrafluoroborate analogues were obtained by a simple stirring reaction with ammonium tetrafluoroborate followed by extraction into dry dichloromethane, whereas BMIMPF<sub>6</sub> was synthesized by stirring the bromide salts with hexafluorophosphoric acid at low temperature followed by extraction into dry dichloromethane. All the ILs were charcoaled with distilled methanol. The solvent was removed in the rotary evaporator and finally the ILs were dried in a vacuum oven for 72 h at  $60^\circ\text{C}$ . The purified ILs were characterized by NMR spectroscopic, mass-spectrometric, and elemental analysis.

**Preparation of the ionogels and organogels:** All the molecules were dissolved in ILs or the corresponding IL-based systems were placed in a glass vial (i.d.: 10 mm) and irradiated in a microwave oven (320 W) for 5–10 s depending on the dissolution of the material. The solutions were cooled (undisturbed) to room temperature. After 30 min, the formation of ionogels was verified by checking the stability of the gel under gravitation by inversion of the glass vial. Organogels were prepared by placing the molecules in organic solvents and slowly heating until the solid completely dissolved. The solutions were cooled to room temperature and formation of gel was verified after 1 h to be stable to inversion by inverting the glass vial.

**Determination of the gel-to-sol transition temperature ( $T_{\text{gel}}$ ):** The gel-to-sol transition temperature was determined by keeping a glass vial containing an ionogel (i.d.: 10 mm) in an oil bath and slowly raising the temperature at a rate of  $2^\circ\text{C min}^{-1}$ . The vial containing the ionogel was inverted in between to check the “stable-to-inversion” property of the gel. The temperature ( $\pm 0.5^\circ\text{C}$ ) at which the gel melts and showed gravitational flow was designated as  $T_{\text{gel}}$ .

**DSC:** DSC was carried out on a Perkin-Elmer Diamond DSC. Gel **1c** (1.3% w/v; 35 mg) in BMIMBr (10% H<sub>2</sub>O, w/v) was placed in a large-volume capsule (LVC) and sealed. The sample LVC pan was placed in the DSC apparatus together with an empty LVC pan as a reference. The pans were cooled to  $20^\circ\text{C}$  and aged for 30 min at this temperature. Heating scans were recorded from  $20$  to  $90^\circ\text{C}$  at a scan rate of  $1^\circ\text{C min}^{-1}$ .

**Microscopic study:** Field emission scanning electron microscopy (FESEM) images were obtained on a JEOL-6700F microscope. The ionogel at MGC was washed with water five times to ensure complete removal of the ionic liquid.<sup>[1a]</sup> A very small amount of the semisolid gel was mounted on a piece of cover slip and SEM images were taken.

**FTIR measurements:** FTIR measurements of the gelators in  $\text{CHCl}_3$  solution and ionogels in BMIMBF<sub>4</sub>, BMIMBr with 10% D<sub>2</sub>O were carried out in a Perkin-Elmer Spectrum 100 FTIR spectrometer with KBr pellets and in a 1-mm CaF<sub>2</sub> cell, respectively.

**NMR measurements:** IL-induced concentration-dependent  $^1\text{H NMR}$  spectra of **1c** were taken on an AVANCE 300 MHz (Bruker) spectrometer. The molecule was initially dissolved in deuterated dimethyl sulfoxide ( $[\text{D}_6]\text{DMSO}$ ) and the ionic liquid content was gradually increased.

**XRD:** A Seifert XRD3000P diffractometer was used with  $\text{Cu}_{\text{K}\alpha}$  radiation as the source ( $\alpha = 0.15406$  nm) and a voltage and current of 40 kV and 30 mA. The sample was put on a glass slide and XRD analysis was performed in a wide-angle region  $10\text{--}60^\circ$ .

**Fluorescence spectroscopy:** The emission spectra of IL solutions (BMIMBr + 10% H<sub>2</sub>O) containing gelator molecule **1c** and **3c** at different concentration were recorded on a Varian Cary Eclipse luminescence spectrometer. The solutions were excited at  $\lambda = 320$  nm. The excitation and emission slit widths were 10 and 10 nm, respectively. The emission spectra of the IL (BMIMBr, 10% H<sub>2</sub>O) and ionogel **1c** in IL (BMIMBr, 10% H<sub>2</sub>O) were recorded at different excitation wavelengths that ranged from  $\lambda = 280$  to  $400$  nm at intervals of 10 nm. The excitation and emission slit widths were 5 and 5 nm, respectively.

**Synthesis of titanium dioxide nanoparticles:** Gelator molecule **1c** (7.5 mg) was dissolved in BMIMBr (500  $\mu$ L, containing 10% water), irradiated in a microwave, and cooled to prepare the ionogel. Titanium tetraisopropoxide (25  $\mu$ L) was added to this ionogel, and water (500  $\mu$ L) was added after half an hour. The reaction mixture was stirred at room temperature for 48 h. The resulting material was filtered, washed several times with water, and calcined at 200 °C for 2 h followed by 500 °C for another 2 h to ensure that no organic portion was left. In a parallel set of experiments, the procedure was repeated under nonstirring conditions. Simultaneous experiments with the gelator below MGC and without gelators were performed by using similar protocols. The white powder was used for FESEM and XRD studies. For AFM, the white powder was taken in HPLC-grade ethanol and sonicated for 30 min. This suspended solution (10  $\mu$ L) was put on a silicon wafer, which was dried under vacuum and used for taking AFM images in a noncontact mode (Veeco, modelAP0100).

**Dye adsorption:** An aqueous solution (3 mL) of crystal violet and naphthol blue black (0.01 mM stock) was taken in two glass vials. Organogel (toluene; 100  $\mu$ L) and ionogel of **1c** (BMIMPF<sub>6</sub>; 2.0%, w/v; 4 mg of the gelator) was added to this solution. As a control experiment, the IL (BMIMPF<sub>6</sub>; 100  $\mu$ L) was added to the aqueous solution of dye. Time-dependent adsorptions of the dyes were monitored by using a Cary-50 UV/Vis spectrophotometer (Varian).<sup>[27]</sup>

## Acknowledgements

P.K.D. is thankful to the Department of Science and Technology (India) for financial assistance through a Ramanna Fellowship (No. SR/S1/RFP-C/04/2006). S.D., D.D., and A.D. acknowledge the Council of Scientific and Industrial Research, India for their Research Fellowships.

- [1] a) K. Hanabusa, H. Fukui, M. Suzuki, H. Shirai, *Langmuir* **2005**, *21*, 10383; b) N. Kimizuka, T. Nakashima, *Langmuir* **2001**, *17*, 6759; c) L. Tan, X. Dong, H. Wang, Y. Yang, *Electrochem. Commun.* **2009**, *11*, 933; d) N. Mohmeyer, D. Kuang, P. Wang, H.-W. Schmidt, S. M. Zakeeruddin, M. Grätzel, *J. Mater. Chem.* **2006**, *16*, 2978; e) M. A. Firestone, J. A. Dzielawa, P. Zapol, L. A. Curtiss, S. Seifert, M. L. Dietz, *Langmuir* **2002**, *18*, 7258; f) K. Lunstrook, K. Driesen, P. Nockemann, C. G. Walrand, K. Binnemans, S. Bellayer, J. L. Bideau, A. Vioux, *Chem. Mater.* **2006**, *18*, 5711; g) S. J. Craythorne, K. Anderson, F. Lorenzini, C. McCausland, E. F. Smith, P. Licence, A. C. Marr, P. C. Marr, *Chem. Eur. J.* **2009**, *15*, 7094–7100; h) M.-A. Néouze, J. L. Bideau, P. Gaveau, S. Bellayer, A. Vioux, *Chem. Mater.* **2006**, *18*, 3931; i) R. T. Carlin, J. Fuller, *Chem. Commun.* **1997**, 1345; j) K. Prasad, Y. Kaneko, J. Kadokawa, *Macromol. Biosci.* **2009**, *9*, 376.
- [2] a) F. D'Anna, S. L. Marca, P. L. Meo, R. Noto, *Chem. Eur. J.* **2009**, *15*, 7896–77902; b) M. J. Earle, K. R. Seddon, *Pure Appl. Chem.* **2000**, *72*, 1391; c) T. Welton, *Chem. Rev.* **1999**, *99*, 2071; d) S. Baj, A. Chrobok, S. Derfla, *Green Chem.* **2006**, *8*, 292; e) P. Wasserscheid, T. Welton, *Ionic Liquids in Synthesis*, Wiley-VCH, Weinheim, **2003**; f) P. G. Rickert, M. R. Antonio, M. A. Firestone, K.-A. Kubatko, T. Szreder, J. F. Wishart, M. L. Dietz, *J. Phys. Chem. B* **2007**, *111*, 4685; g) D. Das, A. Dasgupta, P. K. Das, *Tetrahedron Lett.* **2007**, *48*, 5635.
- [3] a) C. P. Mehnert, R. A. Cook, C. Dispenziere, M. Afework, *J. Am. Chem. Soc.* **2002**, *124*, 12932; b) D. Zhao, M. Wu, Y. Kou, E. Min, *Catal. Today* **2002**, *74*, 157; c) V. Calò, A. Nacci, A. Monopoli, P. Cotugno, *Chem. Eur. J.* **2009**, *15*, 1272.
- [4] a) M. Yamanaka, T. Nakagawa, R. Aoyama, T. Nakamura, *Tetrahedron* **2008**, *64*, 11558; b) K. J. C. van Bommel, C. van der Pol, I. Muizebelt, A. Friggeri, A. Heeres, A. Meetsma, B. L. Feringa, J. van Esch, *Angew. Chem.* **2004**, *116*, 1695; *Angew. Chem. Int. Ed.* **2004**, *43*, 1663; c) M. Suzuki, K. Hanabusa, *Chem. Soc. Rev.* **2009**, *38*, 967; d) S. Debnath, A. Shome, S. Dutta, P. K. Das, *Chem. Eur. J.* **2008**, *14*, 6870; e) T. Kar, S. Debnath, D. Das, A. Shome, P. K. Das, *Langmuir* **2009**, *25*, 8639; f) M. Suzuki, T. Nigawara, M. Yumoto, M. Kimura, H. Shirai, K. Hanabusa, *Org. Biomol. Chem.* **2003**, *1*, 4124; g) D. Batra, D. N. T. Hay, M. A. Firestone, *Chem. Mater.* **2007**, *19*, 4423; h) N. Mohmeyer, H.-W. Schmidt, *Chem. Eur. J.* **2005**, *11*, 863; i) M. Suzuki, Y. Nakajima, M. Yumoto, M. Kimura, H. Shirai, K. Hanabusa, *Org. Biomol. Chem.* **2004**, *2*, 1155; j) A. Pal, Y. K. Ghosh, S. Bhattacharya, *Tetrahedron* **2007**, *63*, 7334; k) A. M. Bieser, J. C. Tiller, *Chem. Commun.* **2005**, 3942–3944.
- [5] a) S. Bellayer, L. Viau, Z. Tebby, T. Toupance, J. L. Bideau, A. Vioux, *Dalton Trans.* **2009**, 1307; b) M. A. Firestone, M. L. Dietz, S. Seifert, S. Trasobares, D. J. Miller, N. J. Zaluzec, *Small* **2005**, *1*, 754; c) D. Batra, S. Seifert, L. M. Varela, A. C. Y. Liu, M. A. Firestone, *Adv. Funct. Mater.* **2007**, *17*, 1279.
- [6] a) S. Tamaru, S. Uchino, M. Takeuchi, M. Ikeda, T. Hatano, S. Shin-kai, *Tetrahedron Lett.* **2002**, *43*, 3751; b) B. Xing, C.-W. Yu, K.-H. Chow, P.-L. Ho, D. Fu, B. Xu, *J. Am. Chem. Soc.* **2002**, *124*, 14846; c) D. Das, A. Dasgupta, S. Roy, R. N. Mitra, S. Debnath, P. K. Das, *Chem. Eur. J.* **2006**, *12*, 5068.
- [7] a) R. N. Mitra, D. Das, S. Roy, P. K. Das, *J. Phys. Chem. B* **2007**, *111*, 14107; b) S. Roy, A. Dasgupta, P. K. Das, *Langmuir* **2007**, *23*, 11769.
- [8] S. Dutta, A. Shome, S. Debnath, P. K. Das, *Soft Matter* **2009**, *5*, 1607.
- [9] a) W. Lu, A. G. Fadeev, B. Qi, E. Smela, B. R. Mattes, J. Ding, G. M. Spinks, J. Mazurkiewicz, D. Zhou, G. G. Wallace, D. R. MacFarlane, S. A. Forsyth, M. Forsyth, *Science* **2002**, *297*, 983; b) B. M. Quinn, Z. Ding, R. Moulton, A. J. Bard, *Langmuir* **2002**, *18*, 1734.
- [10] a) P. Poizot, S. Laruelle, S. Grugeon, L. Dupont, J.-M. Tarascon, *Nature* **2000**, *407*, 496; b) A. Fiedler, D. Schröder, S. Shaik, H. Schwarz, *J. Am. Chem. Soc.* **1994**, *116*, 10734; c) E. Palomares, J. N. Clifford, S. A. Haque, T. Lutz, J. R. Durrant, *J. Am. Chem. Soc.* **2003**, *125*, 475; d) M. Thelakkat, C. Schmitz, H.-W. Schmidt, *Adv. Mater.* **2002**, *14*, 577.
- [11] a) N. Mohmeyer, H.-W. Schmidt, *Chem. Eur. J.* **2007**, *13*, 4499; b) M. Suzuki, T. Sato, A. Kurose, H. Shirai, K. Hanabusa, *Tetrahedron Lett.* **2005**, *46*, 2741.
- [12] a) C.-C. Lin, A. T. Metters, *Adv. Drug Delivery Rev.* **2006**, *58*, 1379; b) L. A. Estroff, A. D. Hamilton, *Chem. Rev.* **2004**, *104*, 1201; c) K. Y. Lee, D. J. Mooney, *Chem. Rev.* **2001**, *101*, 1869; d) J. C. Tiller, *Angew. Chem.* **2003**, *115*, 3180–3183; *Angew. Chem. Int. Ed.* **2003**, *42*, 3072–3075; e) J. Sorber, G. Steiner, V. Schulz, M. Günther, G. Gerlach, R. Salzer, K.-F. Arndt, *Anal. Chem.* **2008**, *80*, 2957.
- [13] a) M. Moniruzzaman, P. R. Sundararajan, *Langmuir* **2005**, *21*, 3802; b) J. H. Jung, S. Shinkai, T. Shimizu, *Chem. Eur. J.* **2002**, *8*, 2684; c) A. Shome, S. Debnath, P. K. Das, *Langmuir* **2008**, *24*, 4280; d) S. Bhattacharya, Y. K. Ghosh, *Chem. Commun.* **2001**, 185.
- [14] M. de Loos, J. H. van Esch, R. M. Kellogg, B. L. Feringa, *Tetrahedron* **2007**, *63*, 7285.
- [15] J. Kyte, R. F. Doolittle, *J. Mol. Biol.* **1982**, *157*, 105.
- [16] a) F. M. Menger, K. L. Caran, *J. Am. Chem. Soc.* **2000**, *122*, 11679; b) S. Mukhopadhyay, U. Maitra, I. Ra, G. Krishnamoorthy, J. Schmidt, Y. Talmon, *J. Am. Chem. Soc.* **2004**, *126*, 15905.
- [17] a) Y. Zhao, G. Yuan, P. Roche, M. Leclerc, *Polymer* **1995**, *36*, 2211; b) B. Jeong, Y. H. Bae, S. W. Kim, *Macromolecules* **1999**, *32*, 7064.
- [18] a) H. Yang, T. Yi, Z. Zhou, Y. Zhou, J. Wu, M. Xu, F. Li, C. Huang, *Langmuir* **2007**, *23*, 8224; b) G. John, J. H. Jung, M. Masuda, T. Shimizu, *Langmuir* **2004**, *20*, 2060; c) C. Wang, D. Zhang, D. Zhu, *Langmuir* **2007**, *23*, 1478; d) A. M. Bieser, J. C. Tiller, *J. Phys. Chem. B* **2007**, *111*, 13180; e) K. Yabuuchi, E. M. Owusu, T. Kato, *Org. Biomol. Chem.* **2003**, *1*, 3464; f) M. Suzuki, Y. Nakajima, M. Yumoto, H. Shirai, K. Hanabusa, *Langmuir* **2003**, *19*, 8622; g) C.-C. Tsou, S.-S. Sun, *Org. Lett.* **2006**, *8*, 387; h) B. Escuder, M. Llusar, J. F. Miravet, *J. Org. Chem.* **2006**, *71*, 7747.
- [19] F. H. Billiot, M. McCarroll, E. J. Billiot, J. K. Rugutt, K. Morris, I. M. Warner, *Langmuir* **2002**, *18*, 2993.
- [20] H. Itagaki, H. Fukiishi, T. Imai, M. Watase, *J. Polym. Sci. Part B* **2005**, *43*, 680.
- [21] a) A. Paul, P. K. Mandal, A. Samanta, *J. Phys. Chem. B* **2005**, *109*, 9148; b) P. K. Mandal, A. Samanta, *J. Phys. Chem. B* **2005**, *109*, 15172; c) A. Paul, P. K. Mandal, A. Samanta, *Chem. Phys. Lett.* **2005**, *402*, 375.

- [22] R. N. Mitra, P. K. Das, *J. Phys. Chem. C* **2008**, *112*, 8159.
- [23] a) Y. Zhou, M. Antonietti, *J. Am. Chem. Soc.* **2003**, *125*, 14960; b) N. Yamanaka, R. Kawano, W. Kubo, N. Masaki, T. Kitamura, Y. Wada, M. Watanabe, S. Yanagida, *J. Phys. Chem. B* **2007**, *111*, 4763.
- [24] K. S. Yoo, T. G. Lee, J. Kim, *Microporous Mesoporous Mater.* **2005**, *84*, 211.
- [25] a) P. K. Malik, *J. Hazard. Mater.* **2004**, *113*, 81; b) A. Bhatnagar, A. K. Jain, *J. Colloid Interface Sci.* **2005**, *281*, 49.
- [26] R. S. Varma, V. V. Namboodiri, *Chem. Commun.* **2001**, 643.
- [27] The gelation properties of **1c** and **3c** in organic solvents and the hydrophilic IL mixture, FESEM images of the TiO<sub>2</sub> nanoparticles, and the UV/Vis spectroscopic study of the time-dependent removal of naphthol blue black and crystal violet with an organogel (**1c** in toluene) are given in the Supporting Information.

Received: July 10, 2009

Revised: September 16, 2009

Published online: December 17, 2009